Simulation of High-Speed Interconnects in a Multilayered Medium in the Presence of Incident Field

Ihsan Erdin, Roni Khazaka, *Student Member, IEEE,* and Michel S. Nakhla, *Fellow, IEEE*

***Abstract*—Simulation of high-speed circuits and interconnects in the presence of incident electromagnetic interference is becoming an important step in the design cycle. An accurate and efficient method for the analysis of incident field coupling to traces in inhomogeneous medium is described. The method is based on the application of the physical optics technique. An interconnect circuit simulation stamp is derived. This stamp provides an easy link to current simulators and to recently developed model reduction techniques. In addition to accounting for the inhomogeneity of the medium, this method provides significant in computational efficiency improvement over conventional approaches.**

***Index Terms*—Circuit simulation, electromagnetic susceptibility, model reduction, physical optics, transmission lines.**

I. Introduction

SIGNAL integrity degradation due to interconnect effects is currently an important performance limiting factor in high-speed systems [1]–[9]. In addition to the effects of crosstalk, delay, and reflections, electrically long interconnects function as spurious antennas to pick up emissions from other nearby electronic systems. The coupled fields may cause signal degradation and false switching which makes signal integrity a challenging task for high-speed designers.

Simulation of interconnects with incident field coupling, requires a stamp which can be included in the modified nodal analysis (MNA) [10] circuit equations. For interconnect analysis in the absence of EMI, this stamp is derived from the solution of the telegrapher's equations. The same applies for the case of incident field coupling to interconnects, but with additional distributed sources added to the telegrapher's equations. These forcing functions depend on the incident field and the geometry of the structure. The presence of a layered dielectric structure would therefore have a significant effect on the value of these forcing functions. Various simulation techniques have been proposed for the analysis of incident field coupling to interconnects [11]–[27]. In general, these techniques treat the medium surrounding the interconnects as homogeneous when performing incident field calculations. The inhomogeneity is only accounted for in calculation of the per-unit length parameters of the interconnects. Imposing such conditions for inhomogeneous structures introduces errors in the results at high frequencies, as demonstrated in this paper. Accounting for the inhomogeneity of the layered medium requires the calculation of the fields in each layer separately. This computation can be done using full wave techniques such as the finite element method (FEM) or the finite-difference time-domain (FDTD) method. These techniques, however, require prohibitively high central processing unit (CPU) and memory resources.

In this paper, an efficient method is proposed for the accurate simulation of the traces in a planarly layered inhomogeneous medium. The fields in the layered medium are calculated using the physical optics technique. Based on the field distribution, a stamp for circuit simulation is then derived. For a large class of practical cases, this technique provides an accuracy similar to that of the full wave techniques while requiring a fraction of the CPU cost. The main advantages of this technique are summarized below.

1) The effect of the layered dielectric is accounted for. This provides a significant improvement in accuracy over the homogeneous assumption which is commonly found in the literature.
2) The field calculation is done without relying on computationally expensive full wave methods.
3) The resulting forcing functions are put in a similar form to those resulting from the homogeneous assumption. This allows the use of currently developed simulation techniques for the analysis of the transmission line stamp.
4) The form of the transmission line stamp is compatible with recently developed model reduction techniques such as complex frequency hopping (CFH) [28], [29]. These techniques provide orders of magnitude of CPU improvement over conventional SPICE analysis.

This paper is organized as follows. In Section II, the transmission line equations with incident field excitation are formulated for the interconnects in a layered medium. The use of physical optics to compute the fields within a planarly layered medium is presented in Section III. In Section IV, the circuit simulation aspects for solving the proposed transmission line stamp are discussed. A brief overview of the full wave method used to validate the accuracy of the physical optics model is presented in Section V. In Section VI, numerical examples and comparison with full wave analysis are presented.

Manuscript received March 30, 1998; revised September 27, 1998. This work was supported in part by Defence Research Establishment Ottawa (DREO) and by Communication and Information Technology Ontario (CITO).

The authors are with the Department of Electronics, Carleton University, Ottawa, Ont. K1S 5B6, Canada.

Publisher Item Identifier S 0018-9480(98)09212-6.

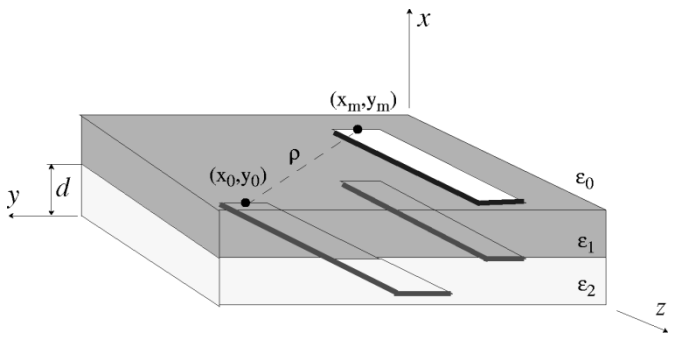

Fig. 1. A layered PCB structure with conducting traces.

II. External Field Coupling to Transmission Lines in Inhomogeneous Medium

In this section, expressions of the forcing functions will be presented for incident field coupling to transmission lines in a multilayered medium. For conductors extending in the z-direction, the transmission line equations with an incident field excitation are given as [12]–[14]

$$\frac{\partial}{\partial z}V(z)+s\boldsymbol{L}I(z)+\boldsymbol{R}I(z) = -\frac{\partial}{\partial z}\int_{\rho(x,y)} E_t^{\text{inc}}(\rho,z)\,d\rho + E_z^{\text{inc}}(x_m,y_m,z) - E_z^{\text{inc}}(x_0,y_0,z) \tag{1}$$

$$\frac{\partial}{\partial z}I(z)+GV(z)+s\boldsymbol{C}V(z) = -\boldsymbol{G}\int_{\rho(x,y)} E_t^{\text{inc}}(\rho,z)\,d\rho - s\boldsymbol{C}\int_{\rho(x,y)} E_t^{\text{inc}}(\rho,z)\,d\rho \tag{2}$$

where $\boldsymbol{R},\boldsymbol{L},\boldsymbol{C}$, and $\boldsymbol{G}$ are the per-unit-length resistance, inductance, capacitance, and conductance, respectively, E_t^{inc} and E_z^{inc} are transverse and axial components of the incident field, and ρ is a parameter of x and y in the transverse plane (Fig. 1). In the layered medium, E_t^{inc} and E_z^{inc} will take on different values from those in free space, which can be determined by the physical optics method.

According to physical optics, a plane wave incident on a planarly layered medium undergoes multiple reflections and refractions, which results in two sorts of waves in each layer: 1) transmitted and 2) reflected waves. Assuming the reference conductor is placed at the origin of the coordinate system, those waves can be written as follows [30], [31]:

$$\begin{aligned}\vec{\boldsymbol{E}}^t(x,y,z) &= (A_{x,i}\hat{a}_x + A_{y,i}\hat{a}_y + A_{z,i}\hat{a}_{z,i}\hat{a}_z)\\ &\quad\cdot e^{-ik_{x,i}x}e^{-jk_y y}e^{-yk_z z}\\ \vec{\boldsymbol{E}}^r(x,y,z) &= (B_{x,i}\hat{a}_x + B_{y,i}\hat{a}_y + B_{z,i}\hat{a}_{z,i}\hat{a}_z)\\ &\quad\cdot e^{jk_{x,i}x}e^{-jk_y y}e^{-jk_z z}\end{aligned} \tag{3}$$

where k_i is the wavenumber, A_i and B_i are the amplitudes of the waves traveling in the same direction as the incident and reflected waves, respectively, with the subscript i referring to the layer number. Calculation of the coefficients A_i and B_i in (3) is the objective of the next section. The total field within the ith layer is the sum of the transmitted and reflected fields. In the transverse plane, the total electric field $E_{T,i}$ can be written as follows:

$$\begin{aligned}\vec{\boldsymbol{E}}_{T,i}(x,y,z) &= [(A_{x,i}e^{-jk_{x,i}x} + B_{x,i}e^{jk_{x,i}x})\hat{a}_x\\ &\quad + (A_{y,i}e^{-jk_{x,i}x} - B_{y,i}e^{jk_{x,i}x})\hat{a}_y]e^{-jk_y y}e^{-jk_z z}.\end{aligned} \tag{4}$$

The line integral of the transverse field between the ground trace and the mth trace positioned in the ith layer is written as follows:

$$V(x_m,y_m,z) = \int_{\rho(x,y)} \vec{\boldsymbol{E}}_{T,i}(\rho,z)\,d\vec{\rho}. \tag{5}$$

If the reference and the signal traces do not lie in the same layer, the integration in the transverse plane must include the effect of each layer in between. The solution of (5) yields the transverse component of the forcing function in the ith layer and at the mth conductor position as

$$\begin{aligned}V_t(x_m,y_m,z) &= j\left[\frac{e^{-j(k_{x,i}x_m+k_y y_m)}-1}{k_{x,i}x_m+k_y y_m}(A_{x,i}x_m + A_{y,i}y_m)\right.\\ &\quad\left. - \frac{e^{j(k_{x,i}x_m-k_y y_m)}-1}{k_{x,i}x_m-k_y y_m}(B_{x,i}x_m - B_{y,i}y_m)\right]e^{-jk_z z}.\end{aligned} \tag{6}$$

The longitudinal component of the forcing function E_L can be written in a similar fashion

$$\vec{\boldsymbol{E}}_L(x_m,y_m,z) = (E_{z,i}(x_m,y_m,z) - E_z(x_0,y_0,z))\hat{a}_z \tag{7}$$

where

$$\begin{aligned}E_{z,i}(x_m,y_m,z) &= (A_{z,i}e^{-jk_{x,i}x_m} - B_{z,i}e^{jk_{x,i}x_m})e^{-jk_y y_m}e^{-jk_z z}.\end{aligned} \tag{8}$$

Since the reference conductor is at the origin of the coordinate system ($x_0 = y_0 = 0$), one obtains

$$\begin{aligned}\vec{\boldsymbol{E}}_L(x_m,y_m,z) &= [A_{z,i}(e^{-j(k_{x,i}x_m+k_y y_m)}-1)\\ &\quad - B_{z,i}(e^{j(k_{x,i}x_m-k_y y_m)}-1)]e^{-jk_z z}\hat{a}_z.\end{aligned} \tag{9}$$

Equations (6) and (9) are of the same form as those obtained in [11] for the homogeneous case, except that the field amplitudes A and B in this case depend on frequency. Incorporating these equations to (1) and (2), one obtains

$$\frac{\partial}{\partial z}V(s,z)+s\boldsymbol{L}I(s,z)+\boldsymbol{R}I(s,z) = V_{F,m}(s,z) \tag{10}$$

$$\frac{\partial}{\partial z}I(s,z)+\boldsymbol{G}\boldsymbol{V}(s,z)+s\boldsymbol{C}V(s,z) = I_{F,m}(s,z) \tag{11}$$

where

$$V_{F,m}(s,z) = -\frac{\partial}{\partial z}V_t(x_m,y_m,z) + E_L(x_m,y_m,z) \tag{12}$$

$$I_{F,m}(s,z) = -s\boldsymbol{C}V_t(x_m,y_m,z) - \boldsymbol{G}V_t(x_m,y_m,z). \tag{13}$$

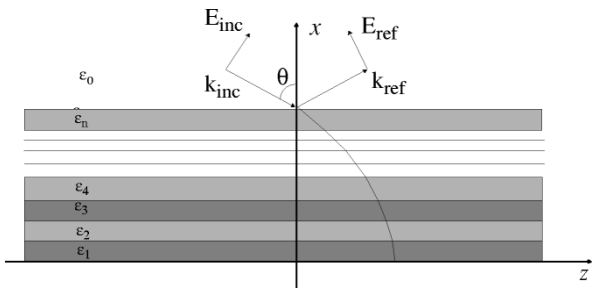

Fig. 2. A general multilayered structure.

III. Calculation of the Fields Within the Layers

In order to solve (10) and (11), the fields in the layered medium must be calculated with conducting traces removed and the dielectric medium in place. For a plane wave whose wavefront is normal to the xz plane and which is incident on a layered medium at an angle θ with respect to the x axis (Fig. 2), (4) takes on the following form:

$$E_{T,i}(x,y,z) = (A_{x,i}e^{-jk_i x\cos\theta_i} + B_{x,i}e^{jk_i x\cos\theta_i})e^{-jk_i z\sin\theta_i}. \quad (14)$$

The boundary conditions at $x = d_i$ are

$$\begin{aligned} &\text{i.} \quad E_{i,z}(d_i,y,z) = E_{i+1,z}(d_i,y,z)\\ &\text{ii.} \quad E_{i,y}(d_i,y,z) = E_{i+1,y}(d_i,y,z)\\ &\text{iii.} \quad H_{i,z}(d_i,y,z) = H_{i+1,z}(d_i,y,z)\\ &\text{iv.} \quad H_{i,y}(d_i,y,z) = H_{i+1,y}(d_i,y,z). \end{aligned} \quad (15)$$

From the Maxwell–Faraday equation, one obtains the following relations:

$$\begin{aligned} H_x &= -\frac{k_z}{\omega\mu}(A_y e^{-jk_x x} + B_y e^{jk_x x})e^{-jk_z z}\\ H_y &= -\frac{k_x}{\omega\mu}(A_y e^{-jk_x x} + B_y e^{jk_x x})e^{-jk_z z}\\ H_y &= \frac{k}{\omega\mu\cos\theta}(A_z e^{-jk_x x} - B_z e^{jk_x x})e^{-jk_z z} \end{aligned} \quad (16)$$

where k_x, k_y, and k_z are the x, y, and z components of the wave vector, respectively. At the boundaries, tangential components of the electric field are continuous, whereas the tangential component of the magnetic field is discontinuous by the amount of surface current density. Assuming a lossless medium, the following basic equations are obtained at each boundary:

$$K_i(A_{y,i}e^{-jk_{x,i}h_i} - B_{y,i}e^{jk_{x,i}h_i}) = A_{y,i+1}e^{-jk_{x,i+1}h_i} - B_{y,i+1}e^{jk_{x,i+1}h_i} \quad (17)$$

$$A_{y,i+1}e^{-jk_{x,i}h_i} - B_{y,i}e^{jk_{x,i}h_i} = A_{y,i}e^{-jk_{x,i+1}h_i} + B_{y,i+1}e^{jk_{x,i+1}h_i} \quad (18)$$

where

$$K_i = \frac{k_{x,i}}{k_{x,i+1}} \quad (19)$$

for TE-polarized waves, and

$$K_i = \frac{k_i\cos\theta_{i+1}}{k_{i+1}\cos\theta_i} \quad (20)$$

for TM-polarized waves. Along with the Snell's law of refraction

$$|k_i|\sin\theta_i = |k_{i+1}|\sin\theta_{i+1} \quad (21)$$

the field amplitudes A and B in (17) and (18) can be solved for and substituted in (6) and (9) to evaluate (12) and (13), respectively.

IV. Linking to Circuit Simulation

The distributed forcing functions can be expressed as

$$F(s,z) = \begin{bmatrix} I_F(s,z)\\ V_F(s,z)\end{bmatrix} \quad (22)$$

where $F(s)$ is the vector representing the distributed sources $V_F(s,z)$ and $I_F(s,z)$ defined in (12) and (13). The telegrapher's equations given in (1) and (2) can be rewritten in a matrix form

$$\frac{d}{dz}\begin{bmatrix}\boldsymbol{V}(z,s)\\ \boldsymbol{I}(z,s)\end{bmatrix} = -(\boldsymbol{D}+s\boldsymbol{E})\begin{bmatrix}\boldsymbol{V}(z,s)\\ \boldsymbol{I}(z,s)\end{bmatrix} + \boldsymbol{F}(z,s) \quad (23)$$

where

$$\boldsymbol{D} = \begin{bmatrix}0 & R\\ G & 0\end{bmatrix} \quad E = \begin{bmatrix}0 & L\\ C & 0\end{bmatrix}. \quad (24)$$

The transmission line stamp is the solution of (23) and can be written as

$$\begin{bmatrix}\boldsymbol{V}(l)\\ \boldsymbol{I}(l)\end{bmatrix} = \boldsymbol{T}(s)\begin{bmatrix}\boldsymbol{V}(0)\\ \boldsymbol{I}(0)\end{bmatrix} + \boldsymbol{b}(S) \quad (25)$$

where the state transition matrix $\boldsymbol{T}(s)$ and the equivalent sources due to the impinging field $\boldsymbol{b}(s)$ are given by

$$T(s) = e^{-\varphi l} = \begin{bmatrix}T_{11} & T_{12}\\ T_{21} & T_{22}\end{bmatrix} \quad (26)$$

$$\boldsymbol{b}(s) = e^{-\varphi l}\int_0^l e^{\varphi z}\boldsymbol{F}(z,s)\,dz \quad (27)$$

where

$$\varphi = \boldsymbol{D} + s\boldsymbol{E}. \quad (28)$$

The above stamp can be directly stenciled in the circuit MNA equations. The advantage of this approach is that the distributed sources $F(z,s)$ have the same form as in the case of homogeneous medium and previously published simulation techniques for the homogeneous case are still applicable with minor modifications for the simulation of multiconductor transmission lines within nonlinear circuit environment. Two general approaches are possible for the simulation. The first is based on determining a time-domain model for each interconnect separately. This approach usually relies on a variation of the method of characteristics [11]. The second approach determines a reduced-order time-domain model of the whole linear subcircuit including the interconnects. It is based on the recently introduced moment matching techniques for circuit simulation such as the complex frequency hopping (CFH) algorithm [28], [29]. This technique allows for very efficient generation of a time-domain macromodel that can be incorporated in a SPICE nonlinear simulation.

The steps of the overall algorithm for simulation of interconnects in the presence of incident field are summarized below.

1) The refracted and reflected fields within each layer are calculated using (17), (18), and (21).
2) The transverse integral and the longitudinal electric field are evaluated using (6) and (9).
3) The forcing functions are determined using (12) and (13).
4) The transmission line stamp and associated lumped equivalent source defined in (27) are computed.
5) The transmission line stamp is linked to circuit simulation using CFH [28] or method of characteristics [11].

V. Validation of the Physical-Optics-Based Model

To validate the results of the physical-optics-based method, the finite difference time-domain method (FDTD) was applied in two separate steps. In the first step, fields in the absence of the traces and with the dielectric medium in place are calculated using the FDTD field solver. In the second step, partial derivatives in (1) and (2) are discretized in space and time and approximated with difference equations. The field values are then substituted in the forcing functions and the following expressions are obtained:

$$\begin{aligned}\frac{1}{\partial z}\left(V_{k+1}^{n}-V_{k}^{n}\right)+\frac{L}{\delta t}\left(I_{k}^{n+(1/2)}-I_{k}^{n-(1/2)}\right)\\ +\frac{R}{2}\left(I_{k}^{n+(1/2)}+I_{k}^{n-(1/2)}\right)\\ =-\frac{1}{\partial z}\left(\int_{\rho(x,y)}E_{T,k+1}^{n}\,d\rho-\int_{\rho(x,y)}E_{T,k}^{n}\,d\rho\right)\\ +\frac{1}{2}\left(E_{L,k+1}^{n}(x_m,y_m,z)+E_{L,k}^{n}(x_m,y_m,z)\right)\\ -\frac{1}{2}\left(E_{L,k+1}^{n}(x_0,y_0,z)+E_{L,k}^{n}(x_0,y_0,z)\right)\end{aligned}\tag{29}$$

$$\begin{aligned}\frac{1}{\partial z}\left(I_{k}^{n+(1/2)}-I_{k-1}^{n+(1/2)}\right)+\frac{C}{\partial t}\left(V_{k}^{n+1}-V_{k}^{n}\right)\\ +\frac{G}{2}\left(V_{k}^{n+1}+V_{k}^{n}\right)\\ =-\frac{C}{\partial t}\left(\int_{\rho(x,y)}E_{T,k}^{n+1}\,d\rho-\int_{\rho(x,y)}E_{T,k}^{n}\,d\rho\right)\\ +\frac{G}{2}\left(\int_{\rho(x,y)}E_{T,k}^{n+1}\,d\rho+\int_{\rho(x,y)}E_{T,k}^{n}\,d\rho\right)\end{aligned}\tag{30}$$

where δz and δt are cell size and time step value, respectively. Equations (29) and (30) are solved in a bootstrapping fashion with appropriate terminal conditions [11]. Considering that this approach was validated in [25] with experimental results, it is especially preferred for the validation of the proposed method in this paper. A summary of the numerical results is presented in Section VI.

VI. Numerical Examples

In this section, the proposed approach is compared with previous techniques where incident field coupling is calculated neglecting the inhomogeneity of the medium. In the discussions and figures below, the latter approach and physical-optics-based model are referred to as Approach I and Approach II, respectively. The test structure whose physical parameters are given in Fig. 3 was taken as a dielectric board sandwiched between two traces. The electrical parameters of the test structure were computed by method of moments. In all examples, azimuthal incidence angle ϕ was kept constant at $-90°$ and longitudinal incidence angle θ was varied between 0° and 90°. In Figs. 4–9, terminations were matched to the line characteristic impedance. The comparison was made in the time domain for an incident field in the form of a Gaussian pulse envelope waveform whose amplitude falls 120 dB below the peak value at 15 GHz. As can be seen from Figs. 4–8, a good agreement is obtained between the proposed physical-optics-based model (Approach II) and the FDTD full wave analysis.

At normal incidence of the incoming field, Approach I does not cause a substantial error. However, as the angle of incidence is declined from the normal to $\theta = 30°$, a large error is observed especially at the far end of the line. Figs. 4 and 5 illustrate this case for an epoxy-glass substrate $(\varepsilon_r = 4.5)$. The error is relatively small for a duroid substrate $(\varepsilon_r = 2.2)$

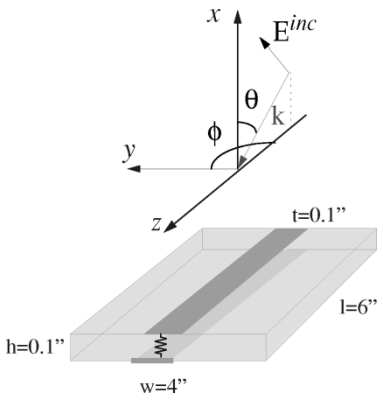

Fig. 3. Test object geometry and coordinate definitions.

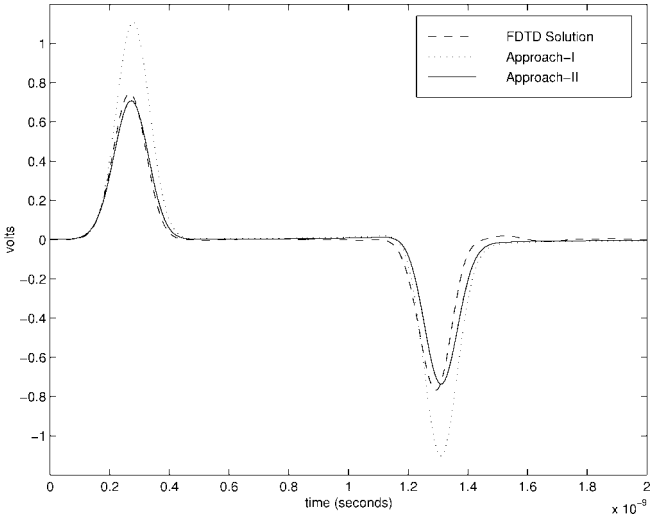

Fig. 4. Coupled voltage waveform at the near end of the line $(\theta = 30°, \varepsilon_r = 4.5)$.

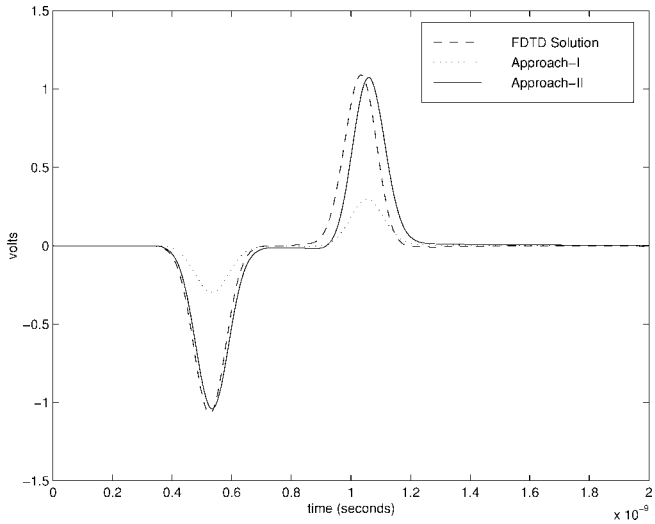

Fig. 5. Coupled voltage waveform at the far end of the line $(\theta = 30^\circ, \varepsilon_r = 4.5)$.

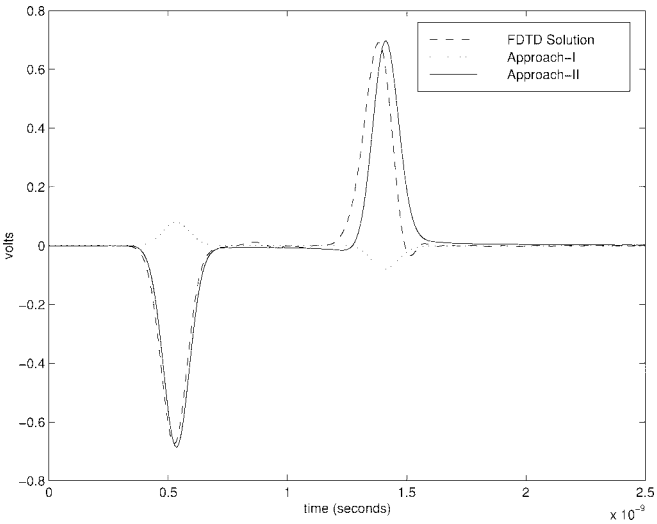

Fig. 7. Coupled voltage waveform at the far end of the line $(\theta = 30^\circ, \varepsilon_r = 11.7)$.

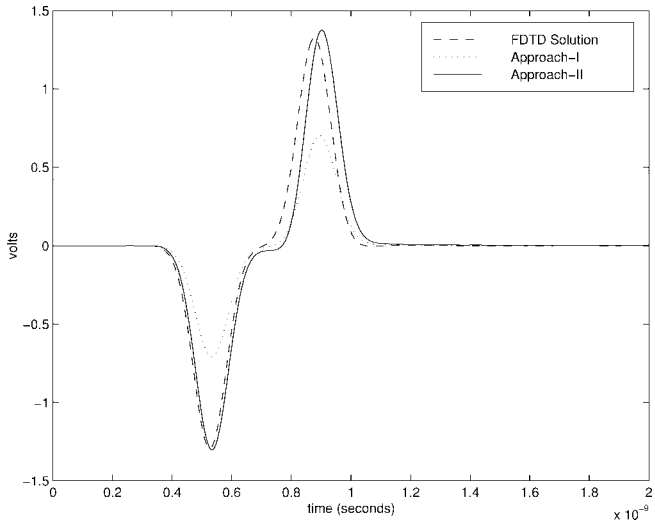

Fig. 6. Coupled voltage waveform at the far end of the line $(\theta = 30^\circ, \varepsilon_r = 2.2)$.

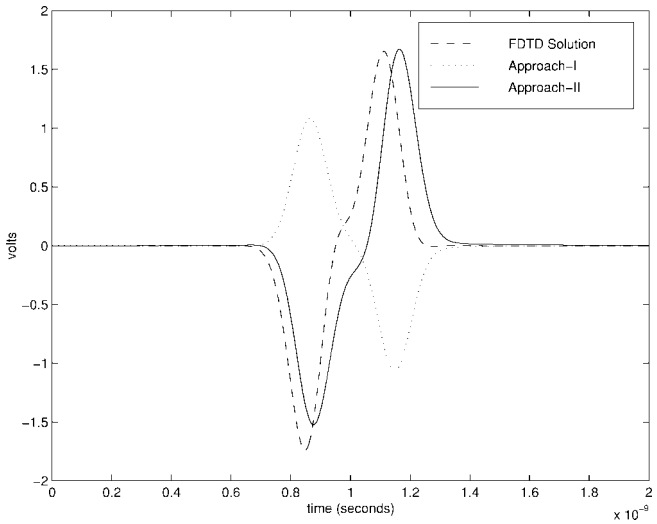

Fig. 8. Coupled voltage waveform at the far end of the $(\theta = 75^\circ, \varepsilon_r = 4.5)$.

whose relative permittivity is, also, comparably small (Fig. 6). For a silicon substrate $(\varepsilon_r = 11.7)$, however, whose relative permittivity is high, a larger error is observed (Fig. 7). As the incidence angle is increased to $\theta = 75^\circ$, the error resulting from Approach I becomes more substantial to the extent that the coupled pulse is inverted compared to the solution obtained from FDTD and proposed physical optics approach (Fig. 8).

The numerical examples clearly point out the shortcomings of Approach I in circuit applications. The reason of this deficiency can be explained as follows. With the first illumination at the near end of the trace, a voltage waveform is excited. Consequently, there are two kinds of waves traveling toward the far end: 1) incident electromagnetic waves in the medium and 2) voltage and current waves on the traces. According to Snell's law of refraction, the axial component of the wavevector is the same in all layers. However, the component in the direction of inhomogeneity depends on the relative permittivity of the medium. If it is not accounted for properly as in Approach II, the results will be erroneous. The field magnitude, on the other hand, is hardly affected unless the edge effects and surface waves begin to dominate at grazing incidence angles. Hence, when an arbitrarily polarized incident field is decomposed to its TE- and TM-polarized parts, the effect of the inhomogeneous medium on the TE-polarized part is not substantial.

As the incidence angle is increased to higher values $(\theta = 85^\circ)$, some deviation between FDTD and physical optics results are observed (Fig. 9). This stems from the fact that the physical optics method is based on the assumption that a layered medium planarly extends to infinity. Hence, edge effects cannot be accounted for and simulation of an endfire excitation based on the proposed method is not possible. Finally, Fig. 10 depicts the case where mismatched near- and far-end terminations were taken as 566 Ω.

To sum up, in a small angular zone close to the horizontal, accuracy of the physical optics results suffer. The width of this angular zone mainly depends on the frequency contents

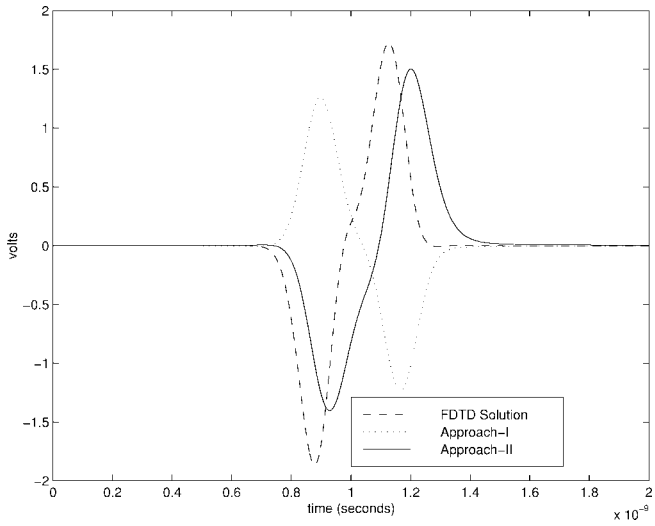

Fig. 9. Coupled voltage waveform at the far end of the line ($\theta = 85°, \varepsilon_r = 4.5$).

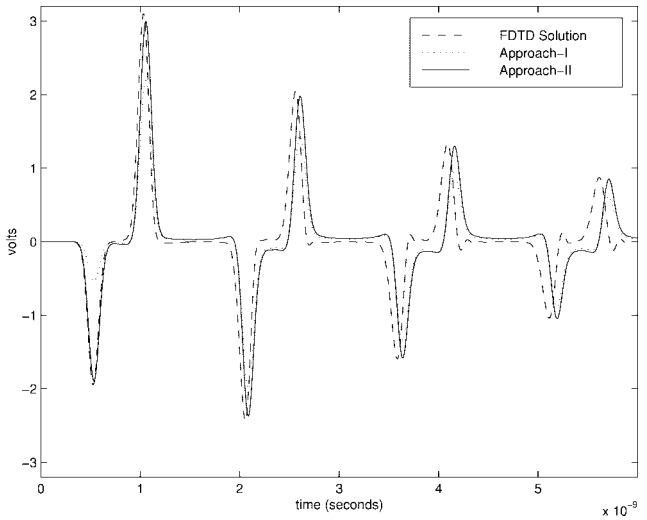

Fig. 10. Coupled voltage waveform at the far end of the line ($\theta = 30°, \varepsilon_r = 4.5$).

of the incident field and the relative permittivity of the layered medium. As demonstrated, for practical circuit applications, the physical optics method matches the full wave techniques successfully over a broad angular region up to a frequency level of 15 GHz.

VII. Conclusions

In this paper, a method is proposed for the analysis of external field coupling to high-speed interconnects in an inhomogeneous dielectric medium. The new method is based on using the physical optics technique for determining the field in the layered medium. For large classes of practical applications, this approach was shown to provide similar accuracy to full wave techniques while requiring a fraction of the CPU and memory resources. The distributed sources due to the external field are put in a similar form to those resulting from the homogeneous assumption. This allows the use of currently developed simulation techniques for the analysis of the transmission line stamp. In addition, the form of the transmission line stamp is compatible with recently developed model reduction techniques. It was also shown that neglecting the inhomogeneity of the dielectric medium leads to erroneous results at high frequencies. The accuracy of the proposed model was verified using the FDTD technique.

Acknowledgment

The authors would like to acknowledge the technical discussions with Dr. S. Kashyap and J. Seregelyi of DREO.

References

[1] A. R. Djordjevic, T. K. Sarkar, and R. F. Harrington, "Analysis of lossy transmission lines with arbitrary nonlinear terminal networks," *IEEE Trans. Microwave Theory Tech.*, vol. MTT-34, pp. 660–666, June 1986.

[2] F. Y. Chang, "The generalized method of characteristics for waveform relaxation analysis of lossy coupled transmission lines," *IEEE Trans. Microwave Theory Tech.*, vol. 37, pp. 2028–2038, Dec. 1989.

[3] W. W. M. Dai (Guest Ed.), "Special issue on simulation, modeling, and electrical design of high-speed and high-density interconnects," *IEEE Trans. Circuits Syst.*, vol. 39 pp. 857–982, Nov. 1992.

[4] J. E. Schutt-Aine and R. Mittra, "Nonlinear transient analysis of coupled transmission lines," *IEEE Trans. Circuits. Syst.*, vol. 36, pp. 959–967, July 1989.

[5] R. Wang and O. Wing, "Transient analysis of dispersive VLSI interconnects terminated in nonlinear loads," *IEEE Trans. Computer-Aided Design*, vol. 11, pp. 1258–1277, Oct. 1992.

[6] N. Orhanovic, P. Wang, and V. K. Tripathi, "Generalized method of characteristics for time domain simulation of multiconductor lossy transmission lines," *Proc. IEEE Symp. Circuits Syst.*, May 1990.

[7] T. K. Tang, M. S. Nakhla, and R. Griffith, "Analysis of lossy multiconductor transmission lines using the asymptotic waveform evaluation technique," *IEEE Trans. Microwave Theory Tech.*, vol. 39, pp. 2107–2116, Dec. 1991.

[8] R. Griffith and M. S. Nakhla, "Mixed frequency/time domain analysis on nonlinear circuits," *IEEE Trans. Computer-Aided Design*, vol. 10, pp. 1032–1043, Aug. 1992.

[9] J. E. Bracken, V. Raghavan, and R. A. Rohrer, "Interconnect simulation with asymptotic waveform evaluation (AWE)," *IEEE Trans. Circuits Syst.*, vol. 39, pp. 869–878, Nov. 1992.

[10] C. W. Ho, A. E. Ruehli, and P. A. Brennan, "The modified nodal approach to network analysis," *IEEE Trans. Circuits Syst.*, vol. CAS-22, pp. 504–509, June 1975.

[11] C. R. Paul, *Analysis of Multiconductor Transmission Lines*. New York: Wiley, 1994.

[12] C. D. Taylor, R. S. Satterwhite, and C. W. Harrison, "The response of a terminated two-wire transmission line excited by a nonuniform electromagnetic field," *IEEE Trans. Antennas Propagat.*, vol. AP-13, pp. 987–989, Nov. 1965.

[13] A. A. Smith, "A more convenient form of the equations for the response of a transmission line excited by nonuniform fields," *IEEE Trans. Electromag. Compat.*, vol. EMC-15, pp. 151–152, Aug. 1973.

[14] C. R. Paul, "Frequency response of multiconductor transmission lines illuminated by an incident electromagnetic field," *IEEE Trans. Microwave Theory Tech.*, vol. MTT-22, pp. 454–457, Apr. 1976.

[15] A. K. Agrawal, H. J. Price, and S. H. Gurbaxani, "Transient response of multiconductor transmission lines excited by a nonuniform electromagnetic field," *IEEE Trans. Electromag. Compat.*, vol. EMC-22, pp. 119–129, May 1980.

[16] Y. Kami and R. Sato, "Circuit-concept approach to externally excited transmission lines," *IEEE Trans. Electromag. Compat.*, vol. EMC-27, pp. 177–183, Nov. 1985.

[17] N. Ari and W. Blumer, "Analytic formulation of the response of a two-wire transmission line excited by a plane wave," *IEEE Trans. Electromag. Compat.*, vol. 30, pp. 437–448, Nov. 1988.

[18] C. R. Paul, "Literal solutions for the time-domain response of a two-conductor transmission line excited by an incident electromagnetic field," *IEEE Trans. Electromag. Compat.*, vol. 37, May 1995.

[19] F. Schlagenhaufer and H. Singer, "Investigation of field excited multiconductor lines with nonlinear loads," in *Proc. 1990 Int. Symp. Electromag. Compat.*, Washington DC, Aug. 1990, pp. 95–99.

[20] R. Khazaka and M. Nakhla, "Analysis of high-speed interconnects in the presence of electromagnetic interference," in *IEEE MTT-S Int. Microwave Symp. Dig.*, June 1996, pp. 1811–1814.
[21] _____, "Analysis of high-speed interconnects in the presence of electromagnetic interference," *IEEE Trans. Microwave Theory Tech.*, vol. 46, pp. 940–947, July 1998.
[22] R. Khazaka, "High-speed interconnect analysis in the presence of incident electromagnetic fields," master's thesis, Carleton Univ., Ottawa, Canada, Dec. 1997.
[23] S. K. Das and W. T. Smith, "Incident field coupling analysis of multiconductor transmission lines using asymptotic waveform evaluation," in *Proc. IEEE Int. Symp. Electromag. Compat.*, Aug. 1996, pp. 265–270.
[24] C. R. Paul, "A SPICE model for multiconductor transmission lines excited by an incident electromagnetic field," *IEEE Trans. Electromag. Compat.*, vol. 36, pp. 342–354, Nov. 1994.
[25] T. Lapahos, J. LoVetri, and J. Seregelyi, "Experimental validation of models for external field coupling to MTL networks with nonlinear junctions," in *1997 North American Radio Science Meeting*, Montreal, Canada, July 1997.
[26] I. Wuyts and D. De Zutter, "Circuit model for plane-wave incidence on multiconductor transmission lines," *IEEE Trans Electromag. Compat.*, vol. 36, pp. 206–212, Aug. 1994.
[27] P. Bernardi, R. Cicchetti, and C. Pirone, "Transient response of a microstrip line circuit excited by an external electromagnetic source," *IEEE Trans. Electromag. Compat.*, vol. 34, pp. 100–108, May 1992.
[28] E. Chiprout and M. Nakhla, "Analysis of interconnect networks using complex frequency hopping (CFH)," *IEEE Trans. Computer-Aided Design*, vol. 14, pp. 186–200, Feb. 1995.
[29] E. Chiprout and M. Nakhla, *Asymptotic Waveform Evaluation and Moment Matching for Interconnect Analysis*. Boston, MA: Kluwer, 1993.
[30] J. A. Kong, *Theory of Electromagnetic Waves*. New York: Wiley, 1975.
[31] K. J. Scott, *Practical Simulation of Printed Circuit Boards and Related Structures*. Taunton, U.K.: Research Studies Press, 1994.

Ihsan Erdin received the B.S. degree in control systems engineering from the Turkish Naval Academy in 1986 and the M.S. degree in electrical engineering from the Middle East Technical University in 1993. He is currently working toward the Ph.D. degree in the Department of Electronics at Carleton University, Ottawa, Ont., Canada.

In 1995, he received a NATO Research Fellowship Award and worked at the Defence Research Establishment Ottawa, Ottawa, Ont., Canada, as a Research Fellow from 1995 to 1996 in the field of external field coupling to electronic systems. His research areas involve EMC/EMI analysis of high-speed interconnects and adaptation of full wave methods to circuit simulation.

Roni Khazaka (S'92) was born on May 6, 1973. He received the B.E. and M.E. degrees from Carleton University, Ottawa, Ont., Canada in 1995 and 1997, respectively. He is currently working toward the Ph.D. degree on the analysis and simulation of radio frequency circuits at the same university.

He has co-authored several papers on high-speed interconnect simulation. His research interests include radio frequency integrated circuits, circuit simulation, EM compatibility, and high-speed interconnects.

Michel S. Nakhla (S'73–M'75–SM'88–F'98) received the M.Eng. and Ph.D. degrees in electrical engineering from Waterloo University, Waterloo, Ont., Canada in 1973 and 1975, respectively.

He is Professor of Electrical Engineering at Carleton University, Ottawa, Ont., Canada. From 1976 to 1988, he was with Bell-Northern Research (currently NORTEL Technology) as the Senior Manager of the computer-aided engineering group. In 1988, he joined Carleton University where he is currently the holder of the Computer-Aided Engineering Senior Industrial Chair established by Bell-Northern Research and the Natural Sciences and Engineering Research Council of Canada. He is the founder of the high-speed CAD research group at Carleton University. He is technical consultant for several industrial organizations and the principal investigator for several major sponsored research projects. His research interests include computer-aided design of VLSI and microwave circuits, modeling and simulation of high-speed interconnects, nonlinear circuits, multidisciplinary optimization, thermal and EM emission analysis, noise analysis, mixed EM/circuit simulation, wavelets, and neural networks.